

# First Experimental Demonstration of Probabilistic Enumerative Sphere Shaping in Optical Fiber Communications

Sebastiaan Goossens<sup>1</sup>, Sjoerd van der Heide<sup>1</sup>, Menno van den Hout<sup>1</sup>, Abdelkerim Amari<sup>1</sup>,  
Yunus Can Gültekin<sup>1</sup>, Olga Vassilieva<sup>2</sup>, Inwoong Kim<sup>2</sup>, Tadashi Ikeuchi<sup>2</sup>, Frans M. J. Willems<sup>1</sup>,  
Alex Alvarado<sup>1</sup>, and Chigo Okonkwo<sup>1</sup>

<sup>1</sup>Department of Electrical Engineering, Eindhoven University of Technology, The Netherlands

<sup>2</sup>Fujitsu Laboratories of America, Inc., 2801 Telecom Parkway, Richardson TX 75082, USA  
s.a.r.goossens@student.tue.nl

**Abstract:** We transmit probabilistic enumerative sphere shaped dual-polarization 64-QAM at 350Gbit/s/channel over 1610km SSMF using a short blocklength of 200. A reach increase of 15% over constant composition distribution matching with identical blocklength is demonstrated.

**Keywords:** Advanced Modulation, Coding and Multiplexing, Coding and forward error correction for optical communications.

## I. Introduction

Fiber optical transmission systems are approaching their capacity limits [1]. In recent years, several techniques have been proposed for increasing spectral efficiency in order to keep up with traffic demands. Within this context, constellation shaping in general—and probabilistic shaping (PS) in particular—have received considerable interest. PS uses uniformly spaced constellation points occurring with different probabilities, which can theoretically provide shaping gains up to 1.53 dB signal-to-noise ratio for the additive white Gaussian noise channel [2]. Even higher gains for the nonlinear fiber optical channel have been reported [3]. Consequently, the development of constellation shaping algorithms integrated with coded modulation has been the subject of intense research [4–7].

Probabilistic amplitude shaping (PAS) [4] integrates a shaping algorithm into an existing bit-interleaved coded modulation (BICM) system [8], as shown in Fig. 1. Constant composition distribution matching (CCDM) was introduced in [4] and is one of the most popular ways of implementing PAS. CCDM is based on a distribution matcher (DM) which requires long blocklengths in order to reach optimum performance [9]. Short blocklengths can be used to reduce the implementation challenges associated with the required arithmetic coding, however, this results in relatively large rate losses [5].

In this paper, an alternative probabilistic shaping algorithm based on enumerative sphere shaping (ESS) is experimentally validated for the first time. ESS was introduced in 1993 [10] and has been recently considered for wireless communications [11]. Very recently, ESS has been introduced to the optical community in [12]. The main result of [12] is that short blocklength ESS outperforms CCDM at the same blocklength, long blocklength CCDM, and uniform. This gain is due to the combination of linear shaping gain and nonlinear tolerance. The results in [12], however, are only based on numerical (split-step Fourier) simulations.

In this paper, 64-ary quadrature amplitude modulation (QAM)-based ESS is experimentally compared against both CCDM and uniform signalling, following the same setup considered in [12]. Both CCDM and ESS indicate good performance with respect to the baseline uniform QAM. However, ESS is demonstrated to outperform CCDM after long-haul optical transmission at equal blocklengths. For a net rate of 350 Gbit/s per channel, gains of 15% translating into 210 km reach increase are demonstrated for ESS with respect to CCDM at a blocklength of 200.

## II. PAS with CCDM and ESS

An amplitude shaper transforms a sequence of  $k$  uniformly distributed input bits into a block of nonuniformly distributed output amplitudes with blocklength  $n$ . The shaping rate  $R_s$  is thus  $R_s = k/n$ . Finite blocklength shaping algorithms suffer from a rate loss which decreases with increasing blocklength [9]. This rate loss is defined as  $R_{\text{loss}} = H(A) - R_s$ , where  $H(A)$  is the entropy of the shaped amplitudes. As the complexity of shaping algorithms is generally linked to blocklength, it is clear that PS algorithms with both short blocklength and low rate loss are not trivial to devise.

Based on arithmetic coding, CCDM maps an input bitstream to any desired output amplitude distribution provided the input bits have equal probabilities. The main property of CCDM is that every shaped block contains the same empirical set of amplitudes, and thus, satisfies the desired amplitude distribution per block. Therefore, it is only able to address a relatively limited set of sequences, and thus, is heavily impacted by rate loss at short blocklengths. ESS, on the other hand, is a shaping algorithm based on sphere coding which *indirectly* induces a nonuniform distribution. In ESS, the output amplitude sequences are bounded-energy sequences, i.e., all sequences satisfy a maximum energy constraint [11, 12]. As a consequence of this, more input bits  $k$  are used for the same blocklength  $n$ , resulting in a much lower rate loss. Using a geometric analogy to further explain the differences between the schemes, CCDM addresses sequences on the shell of a  $n$ -sphere, while ESS addresses all sequences in the CCDM shell as well as all inner shells (with lower energy).

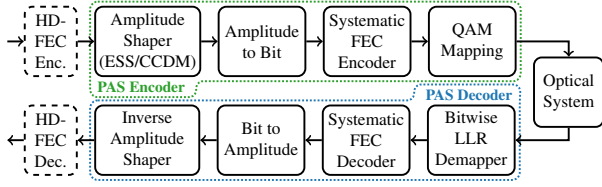


Figure 1: Block diagram of the PAS system under consideration.

Table 1: Parameters for the four systems under consideration.

Name	Shaping	Block length	FEC rate	Net data rate
Uniform	-	-	3/4	9 bit/4D-sym
CCDM-200	CCDM	200	4/5	9 bit/4D-sym
CCDM-3600	CCDM	3600	4/5	9 bit/4D-sym
ESS-200	ESS	200	4/5	9 bit/4D-sym

### III. Experimental Setup

In this paper, all signals are based on 64-QAM. As a baseline, uniform signaling is used with a forward error correction (FEC) rate of 3/4, resulting in a net information rate of 9 bit/4D-sym. For PAS, an FEC rate of 4/5 is employed. The constellation is subsequently shaped to an entropy such that the net information rate is equal to 9 bit/4D-sym (accounting for rate loss). Three shaped schemes are considered: ESS and CCDM with a blocklength of 200, and CCDM with a blocklength of 3600 (a case with negligible rate loss). A summary is shown in Table 1. For the experiment, 20 low-density parity-check (LDPC) blocks of shaped amplitudes are constructed, which are then encoded using the DVB-S2 LDPC code. These bits are mapped to their corresponding symbols following the PAS encoder in Fig. 1.

The sequences are generated offline and contain 216 000 64-QAM symbols, which are pulse-shaped using a root-raised-cosine (RRC) filter with 1% roll-off at 41.79 Gbd and uploaded to a 100-GSa/s digital-to-analog converter (DAC), as shown in Fig. 2 (left). The 1550.116 nm channel under test (CUT) is modulated using an optical-multi-format transmitter (OMFT), which consists of an external cavity laser (ECL), a dual-polarisation IQ-modulator (DP-IQM), an automatic bias controller (ABC) and RF-amplifiers. The multiplexed outputs of 10 ECLs are modulated using a DP-IQM, amplified, split into odd and even channels before being decorrelated by 10 200 symbols (50 m) and 40 800 (200 m) with respect to the CUT, respectively. The CUT, odd and even channels are combined onto the 50-GHz spaced dense wavelength-division multiplexing (DWDM) grid using an optical tunable filter (OTF). Using acoustic optical modulators (AOMs), the signal is circulated in a loop consisting of a loop-synchronised polarisation scrambler (LSPS), a 75-km span of standard single-mode fibre (SSMF), an erbium doped fibre amplifier (EDFA), and an OTF used for gain equalisation. After transmission, the signal is amplified, filtered using a wavelength selective switch (WSS), detected using an intradyne coherent receiver and digitized by an 80-GSa/s real-time oscilloscope. The receiver digital signal processing (DSP) is performed offline and consists of front-end compensation, chromatic dispersion compensation, frequency-offset compensation, and equalization with in-loop phase correction. To reduce the influence from sub-optimal receiver DSP implementation and stability, such as symbol error rate (SER) influence on equalizer feedback performance, training symbols are used for all processed data. On average, 50 sequences have been captured with the oscilloscope resulting in a total of 1000 received LDPC blocks per launch power setting and per distance.

After the conventional DSP, the received symbols are demodulated using a soft-decision bit-wise demapper taking into account the probabilities per symbol. The log-likelihood ratio values are then fed into the LDPC decoder with a maximum of 50 decoding iterations. If shaping is considered, these bits are further processed via the PAS decoder (see Fig. 1). Fig. 2 (right) shows the received constellations after transmission over 375 km for the four cases outlined in Table 1.

### IV. Results

The results are shown in terms of end-to-end bit error rate (BER) and achievable information rate (AIR) for finite length bit-metric decodings (BMDs) with PAS. The latter is defined as (in [5, eq. (26)])

$$\text{AIR}_n = \underbrace{\left[ H(\mathbf{C}) - \sum_{i=1}^6 H(C_i | Y) \right]}_{\text{BMD Rate}} - \underbrace{\left[ H(A) - \frac{k}{n} \right]}_{\text{Rate loss}}, \quad (1)$$

where  $\mathbf{C} = (C_1, C_2, \dots, C_6)$  are the bits at the input of the mapper, and  $Y$  the received symbols after all DSP.

Fig. 3a shows the AIR vs. launch power for a transmission distance of 1500 km and the four cases under consideration. In the linear regime (low input power), Fig. 3a shows that long blocklength CCDM-3600 outperforms ESS-200 and CCDM-200. In the nonlinear regime, ESS-200 exhibits slightly better performance than CCDM with  $n = 3600$ , while the

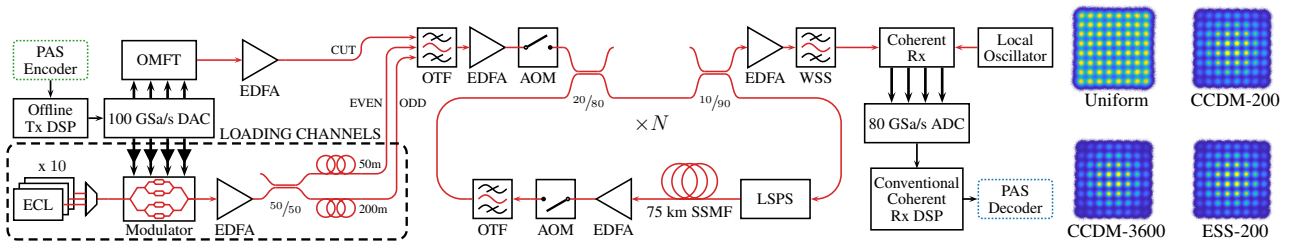


Figure 2: Experimental optical recirculating loop setup (left) and received constellations (right).

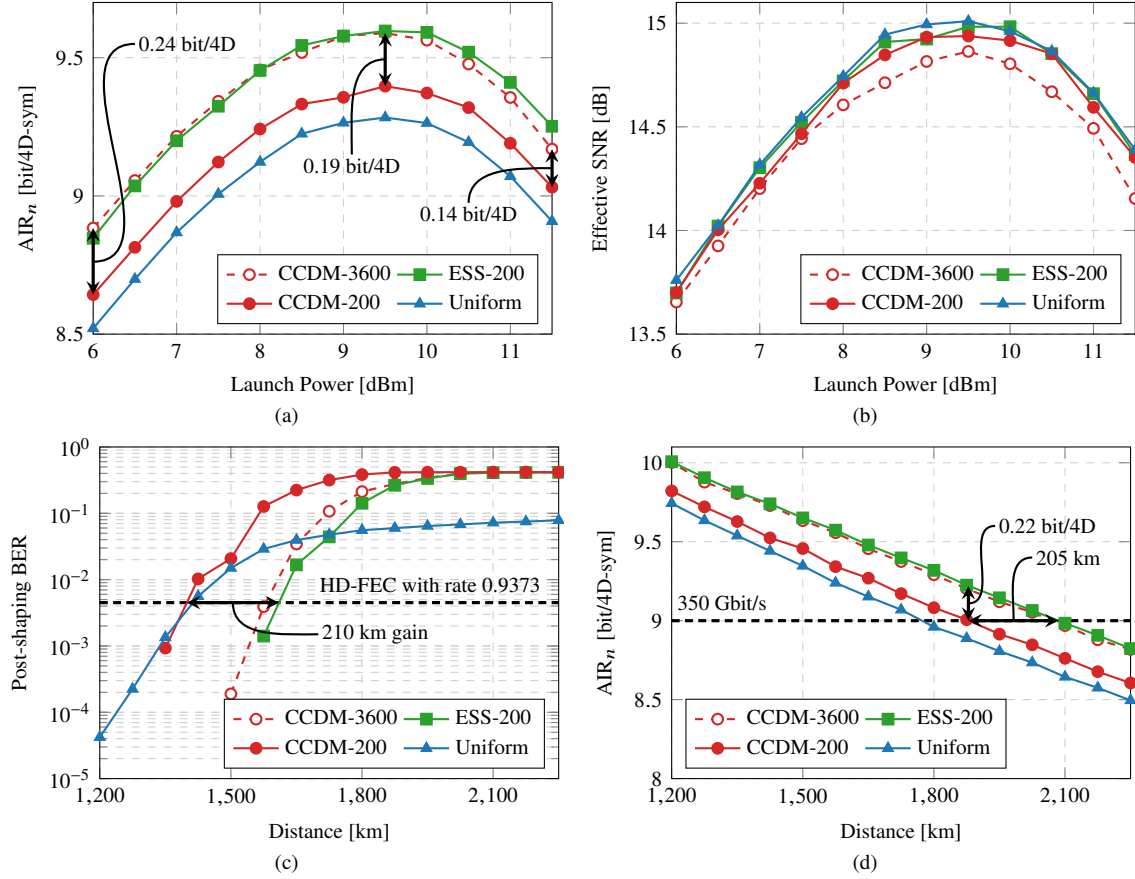


Figure 3: (a)  $AIR_n$  versus launch power at 1500 km (20 spans). (b) Effective SNR versus launch power at 1500 km (20 spans). (c) BER after inverse amplitude shaper versus transmission distance at the optimal launch power of 9.5 dBm. (d)  $AIR_n$  versus transmission distance at the optimal launch power of 9.5 dBm.

performance gap between ESS and CCDDM-200 remains approximately the same at around 0.19 bits/4D-sym. The performance of CCDDM-3600 with respect to CCDDM-200 (illustrated by the black arrows in Fig. 3a) reduces to 0.14 bit/4D. This can be explained by the fact that short blocklengths ESS-200 and CCDDM-200 are more tolerant to nonlinear transmission impairments in comparison to the longer blocklength CCDDM-3600, and is also shown by the effective SNR [13, Eq. 4] in Fig. 3b. This observation has previously been shown in simulations [12]. ESS improves the performance in comparison with CCDDM at the same blocklength due to its lower rate loss, and this gain is independent from the launch power.

BER after shaping decoding is shown in Fig. 3c. An outer hard decision forward error correction (HD-FEC) staircase code with rate 0.9373 [14] that corrects bit errors after LDPC decoding is assumed (see Fig. 1). The BER threshold is  $4.5 \times 10^{-3}$  [14, Fig. 8], which makes ESS-200 15% better in reach (1610 km) compared to CCDDM (1400 km) with the same blocklength, which is an increase of 210 km. Interestingly, ESS-200 is shown to slightly outperform CCDDM-3600. The combination of the rate of this staircase code together with a baudrate of 41.79 GBd and a net information rate of 9 bits/4D-sym results in a total data rate of just over 350 Gbit/s per channel.

Fig. 3d shows the AIR as a function of reach for the optimal launch power of 9.5 dBm. The AIR in Fig. 3d should be interpreted as the reach that an ideal PAS would achieve. For the considered rate (9 bit/4D-sym), ESS-200 offers approximately the same reach as CCDDM-3600. Fig. 3d also shows that CCDDM-200 reaches 1880 km, while ESS-200 reaches 2085 km. This corresponds to a gain of 205 km. While the reach of the systems with non-ideal PAS are smaller (see results in Fig. 3c), the reach increase offered by ESS-200 in comparison with CCDDM-200 is approximately the same (210 km vs. 205 km).

## V. Conclusions

Probabilistic ESS is demonstrated for the first time in an optical transmission experiment. After 1610 km of transmission over SSMF, ESS shows a 15% reach increase over CCDDM at 350 Gbit/s per channel using dual-polarization 64-QAM symbols at a short blocklength regime. The performance of ESS with a significantly lower blocklength is similar or better than that of long blocklength CCDDM. We believe that short blocklength ESS is a promising low-complexity shaping alternative to CCDDM which could find application in next generation optical transceivers.

We acknowledge partial funding from the Dutch Netherlands Scientific Research Organisation (NWO) Gravitation Program on Research Center for Integrated Nanophotonics (Grant Number 024.002.033). The work of A. Alvarado is supported by the NWO via the VIDI Grant ICONIC (project number 15685) and has received funding from the European Research Council (ERC) under the European Union's Horizon 2020 research and innovation programme (grant agreement No 757791). Fraunhofer HHI and ID Photonics are acknowledged for providing the Optical-Multi-Format Transmitter.

## References

1. P. J. Winzer *et al.*, “From scaling disparities to integrated parallelism: A decathlon for a decade,” *JLT* **35**, 1099–1115 (2017).
2. G. Forney *et al.*, “Efficient modulation for band-limited channels,” *IEEE Journal on Selected Areas in Communications* (1984).
3. R. Dar *et al.*, “On shaping gain in the nonlinear fiber-optic channel,” in “IEEE Int. Symposium on Information Theory,” (2014).
4. G. Böcherer *et al.*, “Bandwidth efficient and rate-matched low-density parity-check coded modulation,” *IEEE Trans. on Comm.* (2015).
5. T. Fehenberger *et al.*, “Multiset-partition distribution matching,” *IEEE Transactions on Communications* **67**, 1885–1893 (2019).
6. F. Buchali *et al.*, “Rate adaptation and reach increase by probabilistically shaped 64-qam: An experimental demonstration,” *JLT* (2016).
7. T. Fehenberger *et al.*, “On probabilistic shaping of quadrature amplitude modulation for the nonlinear fiber channel,” *JLT* (2016).
8. L. Szczecinski *et al.*, *Bit-interleaved coded modulation: fundamentals, analysis and design* (Wiley-Blackwell, United States, 2015).
9. P. Schulte *et al.*, “Constant composition distribution matching,” *IEEE Transactions on Information Theory* **62**, 430–434 (2016).
10. F. M. J. Willems *et al.*, “A pragmatic approach to shaped coded modulation,” in “IEEE 1st Symp. on Commun. and Veh. Tech.”, (1993).
11. Y. C. Gültekin *et al.*, “Enumerative Sphere Shaping for Wireless Communications with Short Packets,” arXiv:1903.10244 (2019).
12. A. Amari *et al.*, “Introducing Enumerative Sphere Shaping for Optical Communication Systems with Short Blocklengths,” arXiv:1904.06601 (2019).
13. J. Renner *et al.*, “Experimental comparison of probabilistic shaping methods for unrepeatable fiber transmission,” *Journal of Lightwave Technology* **35**, 4871–4879 (2017).
14. B. P. Smith *et al.*, “Staircase Codes: FEC for 100 Gb/s OTN,” *JLT* **30**, 110–117 (2012).